INTERNATIONAL JOURNAL OF MARITIME TECHNOLOGY
IJMT Vol.20 / Summer& Autumn 2024 (51-60)

Available online at: www. ijmt.ir

Longitudinal Vibration Analysis of Marine Propeller Shaft Using Distributed-Lumped Modeling Technique

Saeed Soheili [1*], Seyyed Esmaeel Hosseini [2], Abdollah Karimi [3]

[1] *Assistant Professor, Department of Mechanical Engineering, Mashhad Branch, Islamic Azad University, Mashhad, Iran. Email: soheili@iau.ac.ir*
[2] *MSc of Mechanical Engineering, Department of Mechanical Engineering, Imam Hossein University, Tehran, Iran. Email: Hosseini.mec62@gmail.com*
[3] *MSc of Mechanical Engineering, Department of Mechanical Engineering, Hakim Sabzevari University, Sabzevar, Iran. Email: abdollah.93.karimi.215@gmail.com*

ARTICLE INFO

Article History
Received: 14 Oct 2024
Accepted: 29 Dec 2024
Available online: 29 Dec 2024

Keywords:
Longitudinal Vibration
Hybrid Modeling
Marine Propeller Shaft
Distributed Element
Lumped Element

ABSTRACT

In this paper, the application of distributed-lumped (hybrid) modeling technique (DLMT) in the modeling of longitudinal (axial) vibration of marine shaft system is investigated. The equation of motion for the longitudinal vibration is solved in new analytical method, and modeled as a series of interconnected distributed and lumped elements. Natural frequencies of a rotor system with various elements are calculated based on the distributed lumped modeling technique (DLMT). The results obtained by this method are compared and verified with the results of other techniques, such as FEM, using ANSYS software, and the mode shapes are also presented. The method is then employed for calculating the natural frequencies of a marine propeller shaft with multiple elements such as different couplings. The results are compared and verified with the frequencies and mode shapes obtained by KissSoft software. It is shown that the presented method provides highly accurate results, while it can be simply and effectively applied to the complicated systems.

1. Introduction

Vibration modeling of industrial systems, especially rotating shafts, is one of the fundamental issues in the engineering design of dynamic systems. Natural frequencies of rotating shafts should not be presented near the working revolution domain. Moreover, the condition monitoring (CM) of sensitive and costly plants such as ships and turbines needs accurate appreciation of different elements and their effects on the whole system vibration [1]. Condition Monitoring for rotating machinery incorporates a wide range of techniques. Developments are continually made with the use of new analysis methods, increased computing power, measurement techniques, and so on. Therefore, developing an accurate vibration model of industrial systems has been one of the main goals of mechanical engineers for decades.

Different analytical solutions are proposed for the simple cases of vibrating systems. However, there is no analytical and precise method for vibration modeling of the complicated systems combined of various shaft and disk elements; such as gears, propellers, pulleys, and so on. In such cases, the proposed techniques widely utilize spring-mass-damper models, such as references [2, 3]; or numerical and approximate methods; such as transfer matrix method (TMM) [4] and finite element method (FEM) [5].

Among different methods of modeling systems such as lumped-lumped modeling technique (LLMT) and distributed-lumped modeling technique (DLMT), or numerical and approximate methods such as transfer matrix method (TMM) and finite element method (FEM), it is clear that the model combined with both the distributed and lumped elements is the best representative of complex and accurate systems.

The distributed- lumped modeling technique (DLMT) was firstly introduced by Whalley [6] for the second order systems. This technique was applied by Aleyaasin et al. [7] for calculating the flexural frequencies of Euler-Bernoulli beams using 4×4 matrices. Recently, DLMT was employed to investigate the flexural vibration of a multi-step turbine shaft using Timoshenko beam theory [8]. The distributed-lumped method can be applied to model the

torsional [9] and flexural [10] vibrations as well. This technique can also be employed to calculate the frequency and time responses in forced systems [9].

For the vibration model of the shaft with FEM, the shaft is discretized in many elements, and the mode shape is approximated by some shape functions. Hence, the procedure introduces approximations in modeling, and finally the accuracy depends on the number of elements. In this method, mass and stiffness matrix orders are 2(n+1)×2(n+1) for n elements.

The transfer matrix method (TMM) also deals with the shaft by discretizing it in many elements. In this method, mode shape is approximated using various separated shaft (field) and disk (point) elements. The shaft element has only elastic properties without mass, and the disk element possesses only mass and inertia moment without elastic characteristics. Therefore, both elements possess approximations in modeling, and finally the accuracy depends on the number of elements as well as other factors.

In contrast with FEM and TMM, the DLMT deals with the shaft as one continuous element with inertia and elastic effects, and since the presented matrix form is based on the main solution of governing equations, no approximation is utilized. Therefore, mathematically or physically; no simplification neither approximation has been taken into account. Another advantage of the DLMT, compared with the FEM, is the reduced size of matrices and equations. The transfer matrix order of the entire system in the DLMT is just 2×2 for longitudinal vibration. Moreover, the boundary conditions (BCs) of the system could be easily applied to the model.

In this study, a method based on the distributed lumped modeling approach is proposed to solve the governing equations of motion for the longitudinal vibration. The method is then employed to model a general three–stage distributed-lumped-distributed system with clamped-free boundary conditions (BCs), which are more common in real systems. To check the correctness and accuracy of the present method, the natural frequencies of the system achieved by this method are compared with those obtained by FEM utilizing ANSYS software. The method is then employed to obtain the frequencies of a marine propulsion system, and the results are compared with KissSoft software outcomes. The mode shapes of propeller shaft system are also presented.

2. The General Distributed-Lumped Model

Generally speaking, systems in the hybrid modeling technique are considered as the combination of two types of elements:

1) The distributed element, which is the main part of shafts and rotors; with the distributed mass or inertia.

2) The lumped element, which is the supplementary part of shafts and rotors; with the concentrated mass or inertia such as disks, gears, propellers, pulleys, and so on.

In this way, a system is considered as a combined set of distributed and lumped elements, in which the final vibration model of system is obtained by setting the distributed and lumped matrices of different parts and combining them together (see Figure 1). Distributed and lumped matrices are formed according to the analytical equations of motion, so this is the highly accurate technique in contrast with the other approximate techniques such as TMM (based on lumped elements), FEM, and so on. Another advantage of this technique is that the continuity conditions between elements are simply satisfied; and only the boundary conditions (BCs) of the system should be applied to the model.

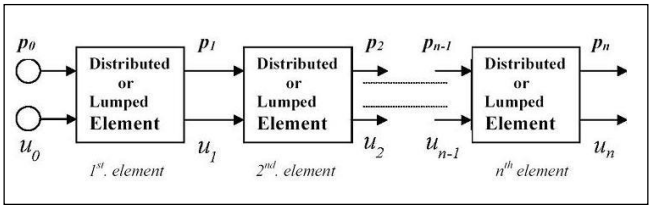

Figure 1. General series representation of a distributed lumped parameter system (hybrid model)

2.1. The Transfer Matrix for Distributed Element

The equations of motion for longitudinal vibration of a thin rod with the density ρ and the modulus of elasticity E can be expressed by the following equations (e.g., see [11, 12]):

$$\frac{\partial p(x,t)}{\partial x} = \rho A \frac{\partial^2 u(x,t)}{\partial t^2} \tag{1}$$

$$\frac{\partial u(x,t)}{\partial x} = \frac{p(x,t)}{AE} \tag{2}$$

Where $u(x,t)$ and $p(x,t)$ are the displacement and internal force functions, x is the distance along a section and t is time.

Differentiating Eq. (2) with respect to x and substituting for $\partial p/\partial x$ in Eq. (1) yields:

$$\frac{\partial^2 u(x,t)}{\partial x^2} = \frac{\rho}{E} \frac{\partial^2 u(x,t)}{\partial t^2} \tag{3}$$

Also, differentiating Eq. (2) twice with respect to t results in:

$$\frac{\partial^3 u(x,t)}{\partial x \partial t^2} = \frac{1}{AE} \frac{\partial^2 p(x,t)}{\partial t^2} \tag{4}$$

Differentiating Eq. (1) with respect to x gives:

$$\frac{\partial^2 p(x,t)}{\partial x^2} = \rho A \frac{\partial^3 u(x,t)}{\partial x \partial t^2} \tag{5}$$

Substituting Eq. (4) into (5) results in:

$$\frac{\partial^2 p(x,t)}{\partial x^2} = \frac{\rho}{E}\frac{\partial^2 p(x,t)}{\partial t^2} \tag{6}$$

Equations (3) and (6) are the main equations of longitudinal vibration. Next, assuming zero initial conditions, Laplace transformation of equations (6) and (3) gives:

$$\begin{aligned} &\frac{\partial^2 p(s,t)}{\partial x^2} - \frac{\rho}{E}s^2 p(s,t) = 0 \\ &\frac{\partial^2 u(s,t)}{\partial x^2} - \frac{\rho}{E}s^2 u(s,t) = 0 \end{aligned} \tag{7}$$

where s is the Laplace transform variable. Eq. (7) can be written in compact form as:

$$\frac{\partial^2 k}{\partial x^2} - \Gamma^2 k = 0 \tag{8}$$

where

$$k = u(x,s) \quad \text{or} \quad p(x,s) \tag{9}$$

and

$$\Gamma = s\sqrt{\frac{\rho}{E}} \tag{10}$$

The general solution of Eq. (8) is given by:

$$k = r_1 e^{\Gamma x} + r_2 e^{-\Gamma x}$$

where:

$$\begin{aligned} e^{\Gamma x} &= \cosh\Gamma x + \sinh\Gamma x \\ e^{-\Gamma x} &= \cosh\Gamma x - \sinh\Gamma x \end{aligned}$$

Therefore we have:

$$k = (r_1 + r_2)\cosh\Gamma x + (r_1 - r_2)\sinh\Gamma x \tag{11}$$

Hence, the solution of Eq. (7) will be:

$$\begin{aligned} p(x,s) &= A\cosh\Gamma x + B\sinh\Gamma x \\ u(x,s) &= C\sinh\Gamma x + D\cosh\Gamma x \end{aligned} \tag{12}$$

The unknown constants of integration A and D are obtained by imposing the boundary conditions at x=0, that is:

$$\begin{aligned} A &= p(0,s) \\ D &= u(0,s) \end{aligned} \tag{13}$$

Next, it remains to find B and C in Eq. (12). Differentiating Eq. (12) with respect to x and substituting for $\partial p/\partial x$ and $\partial u/\partial x$ from Laplace transformation of equations (1) and (2), respectively; gives:

$$\begin{aligned} \rho A s^2 u(x,s) &= A\Gamma\sinh\Gamma x + B\Gamma\cosh\Gamma x \\ \frac{1}{AE}p(x,s) &= C\Gamma\cosh\Gamma x + D\Gamma\sinh\Gamma x \end{aligned} \tag{14}$$

Now putting $x=0$ in Eq. (14) results in:

$$\begin{aligned} B &= sA\sqrt{\rho E}\; u(0,s) = \xi u(0,s) \\ C &= \frac{1}{sA\sqrt{\rho E}}p(0,s) = \frac{1}{\xi}p(0,s) \end{aligned} \tag{15}$$

Hence, the solution of Eq. (7) for the j^{th} element can be expressed in matrix form as:

$$\begin{Bmatrix} p_j(x,s) \\ u_j(x,s) \end{Bmatrix} = \begin{bmatrix} \cosh\Gamma_j x & \xi_j \sinh\Gamma_j x \\ \frac{1}{\xi_j}\sinh\Gamma_j x & \cosh\Gamma_j x \end{bmatrix} \begin{Bmatrix} p_j(0,s) \\ u_j(0,s) \end{Bmatrix}$$

where:

$$\xi_j = sA_j\sqrt{\rho_j E_j}$$

According to Figure 1, for the j^{th} element at x=0 we have:

$$\begin{aligned} p_j(0,s) &= p_{j-1}(s) \\ u_j(0,s) &= u_{j-1}(s) \end{aligned}$$

Therefore:

$$\begin{Bmatrix} p_j(s) \\ u_j(s) \end{Bmatrix} = \begin{bmatrix} \cosh\Gamma_j l_j & \xi_j \sinh\Gamma_j l_j \\ \frac{1}{\xi_j}\sinh\Gamma_j l_j & \cosh\Gamma_j l_j \end{bmatrix} \begin{Bmatrix} p_{j-1}(s) \\ u_{j-1}(s) \end{Bmatrix}$$

Which can be expressed as:

$$\begin{Bmatrix} p \\ u \end{Bmatrix}_j = [T_D]_j \begin{Bmatrix} p \\ u \end{Bmatrix}_{j-1} \tag{16}$$

while:

$$[T_D]_j = \begin{bmatrix} \cosh\Gamma_j l_j & \xi_j \sinh\Gamma_j l_j \\ \frac{1}{\xi_j}\sinh\Gamma_j l_j & \cosh\Gamma_j l_j \end{bmatrix}$$

which is the main transfer matrix for the longitudinal vibration of distributed element in DLMT.

2.2. The Transfer Matrix for Lumped Element

The equation of motion and continuity conditions in Laplace domain of the j^{th} lumped element, which is

exposed to the applied force f in the x-direction are written as:

$$\begin{aligned} p_j(s) - p_{j-1}(s) + f_j(s) &= m_j s^2 u_j(s) \\ u_j(s) &= u_{j-1}(s) \end{aligned} \quad (17)$$

Therefore, Eq. (17) can be expressed in the matrix form as:

$$\begin{Bmatrix} p_j(s) \\ u_j(s) \end{Bmatrix} = \begin{bmatrix} 1 & m_j s^2 \\ 0 & 1 \end{bmatrix} \begin{Bmatrix} p_{j-1}(s) \\ u_{j-1}(s) \end{Bmatrix} + \begin{Bmatrix} -f_j \\ 0 \end{Bmatrix} \quad (18)$$

In the absence of the force f, the matrix form can be expressed as:

$$\begin{Bmatrix} p \\ u \end{Bmatrix}_j = [T_L]_j \begin{Bmatrix} p \\ u \end{Bmatrix}_{j-1} \quad (16)$$

while:

$$[T_L]_j = \begin{bmatrix} 1 & m_j s^2 \\ 0 & 1 \end{bmatrix}$$

which is the main transfer matrix for the longitudinal vibration of lumped element in DLMT.

According to Figure 1, a shaft with multiple elements can be considered as a vibrating system with various types of distributed and lumped elements, and the overall transfer matrix of the system is obtained by putting these elements together, based on their order and physical properties.

3. Illustrative Example and Verification

In this section, the methodology outlined previously is applied to a shaft with a disk on its middle (see Figures 2 and 3), which is a simplified model for common industrial systems. The results are then compared with the FEM solution. The properties of the system considered here are shown in Table 1. As mentioned already, the present method can be used for analyzing systems with any number of distributed and lumped elements without any increasing in difficulty.

Table 1. Properties of the propeller shaft model

Parameter	Quantity
Shaft Overall Length 2L	4 m
Shaft Diameter d	0.150 m
Density of Shaft Material ρ	7800 kg/m^3
Modulus of Elasticity for Shaft E	200 GPa
Shear Modulus of Shaft G	80 GPa
Disk Thickness t	0.080 m
Disk Radius r	1 m
Disk Mass	100 kg
Disk Moment of Inertia	50 kgm^2

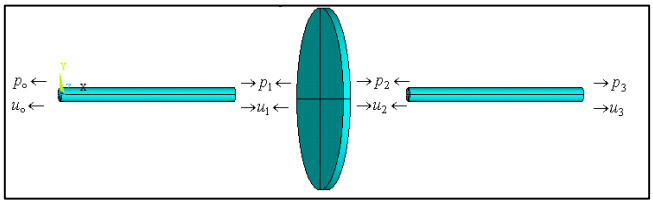

Figure 2. General model of rotating shaft system

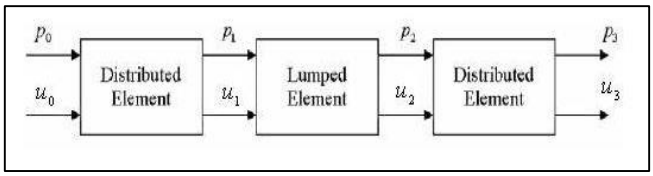

Figure 3. Hybrid model of rotating shaft system

3.1. The DLMT Solution

To represent the main hybrid model of the system, it should be noticed that the system is combined of two distributed and one lumped elements (Figure 3). For the distributed elements 1 and 3 the transfer matrices can be written according to Eq. (16) as:

$$\begin{Bmatrix} p_1 \\ u_1 \end{Bmatrix} = [T_D]_1 \begin{Bmatrix} p_0 \\ u_0 \end{Bmatrix}, \quad \begin{Bmatrix} p_3 \\ u_3 \end{Bmatrix} = [T_D]_3 \begin{Bmatrix} p_2 \\ u_2 \end{Bmatrix} \quad (19)$$

where:

$$[T_D] = \begin{bmatrix} \cosh \Gamma l & \xi \sinh \Gamma l \\ \frac{1}{\xi} \sinh \Gamma l & \cosh \Gamma l \end{bmatrix} \quad (20)$$

In addition, the transfer matrix for the lumped element is:

$$\begin{Bmatrix} p_2 \\ u_2 \end{Bmatrix} = [T_L]_2 \begin{Bmatrix} p_1 \\ u_1 \end{Bmatrix} \quad (21)$$

where:

$$[T_L]_2 = \begin{bmatrix} 1 & m_2 s^2 \\ 0 & 1 \end{bmatrix} \quad (22)$$

Substituting Eq. (19) into (21) yields [10,11]:

$$\begin{Bmatrix} p_3 \\ u_3 \end{Bmatrix} = \begin{bmatrix} \cosh 2\Gamma l + \frac{1}{2} m_2 \xi^{-1} s^2 \sinh 2\Gamma l & \xi \sinh 2\Gamma l + m_2 s^2 \cosh^2 \Gamma l \\ \xi^{-1} \sinh 2\Gamma l + m_2 \xi^{-2} s^2 \sinh^2 \Gamma l & \cosh 2\Gamma l + \frac{1}{2} m_2 \xi^{-1} s^2 \sinh 2\Gamma l \end{bmatrix} \begin{Bmatrix} p_0 \\ u_0 \end{Bmatrix} \quad (23)$$

Equation (23) may be shown in the simple form as follows:

$$\begin{Bmatrix} p_3 \\ u_3 \end{Bmatrix} = [T] \begin{Bmatrix} p_0 \\ u_0 \end{Bmatrix} \quad (24)$$

where:

$$[T]=\begin{bmatrix} \cosh 2\Gamma l+\frac{1}{2}m_2\xi^{-1}s^2\sinh 2\Gamma l & \xi\sinh 2\Gamma l+m_2s^2\cosh^2\Gamma l \\ \xi^{-1}\sinh 2\Gamma l+m_2\xi^{-2}s^2\sinh^2\Gamma l & \cosh 2\Gamma l+\frac{1}{2}m_2\xi^{-1}s^2\sinh 2\Gamma l \end{bmatrix} \quad (25)$$

Equation (25) is the transfer matrix of the overall system relating axial forces and axial displacements of the left and right end of the system.
The Laplace transform variable 's', in general, is the representative of equation $s=\sigma+i\omega$; in which the real part (σ) shows damping, and the imaginary part ($i\omega$) shows vibrating frequency. It is assumed in the present example that $\sigma=0$ and, therefore, Eq. (24) will be altered from Laplace domain into frequency domain by putting $s=i\omega$ [10].

3.2. Numerical Results and Discussions

For each sets of boundary conditions one characteristic equation can be obtained that its solutions will give the natural frequencies of the system.
Assuming that the shaft is clamped at the position zero, and free at the position 3, the boundary conditions will be (see Figure 3):

$$\begin{aligned} u_0 &= 0 \quad (at\ clamped\ end) \\ p_3 &= 0 \quad (at\ \ free\,end) \end{aligned} \quad (26)$$

According to the above relations, Eq. (24) can be arranged as:

$$\begin{Bmatrix} p_0 \\ u_3 \end{Bmatrix}=\begin{bmatrix} \frac{1}{T_{11}} & -\frac{T_{12}}{T_{11}} \\ \frac{T_{21}}{T_{11}} & -\frac{T_{21}T_{12}}{T_{11}}+T_{22} \end{bmatrix}\begin{Bmatrix} p_3 \\ u_0 \end{Bmatrix} \quad (27)$$

where u_0 and p_3, are the inputs and u_3 and p_0 are the outputs of the system.
In this case, the natural frequencies are obtained by plotting u_3/p_3 or u_3/u_0, for instance, as shown in Fig. 4. In this view, the natural frequencies occur at the peaks of the spectrum. From Eq. (27), it is clear that the peaks are the result of denominator approaching zero. Since in all relations T_{11} is the denominator, so the natural frequencies are the roots of T_{11}.
Other than that, putting the relations (26) in Eq. (24) gives:

$$\begin{aligned} T_{11}p_0 &= 0 \\ T_{21}p_0 &= u_3 \end{aligned} \quad (28)$$

The first equation is satisfied when $T_{11}=0$, which is another reason for computing the roots of T_{11} to find the natural frequencies as well. The results for this case are listed in Table 2.

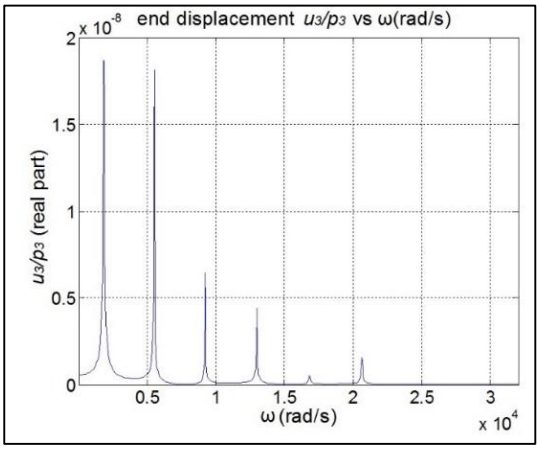

Figure 4. Frequency spectrum for clamped-free BCs (u_3/p_3 vs. ω(rad/s))

Table 2. Natural frequencies of clamped-free rotating system

Frequency (Hz)	f_1	f_2	f_3	f_4	f_5	f_6
DLMT Solution	290	875	1464	2064	2671	3285
FEM Solution	292	881	1480	2085	2704	3321
%Error (FEM with respect to DLMT)	0.690	0.686	1.093	1.017	1.245	1.096

3.3. FEM Solution

To contrast and confirm the results with another method, the finite element method is used to investigate the natural frequencies. The system is modeled by ANSYS software, and meshed using brick 45 (8 nodes 3D) elements (Figure 5). Block Lanczos solver of ANSYS is used in the analysis. The natural frequencies are listed in Table 2. Also the first 4 mode shapes for clamped-free boundary conditions are shown in Figures 6-9.

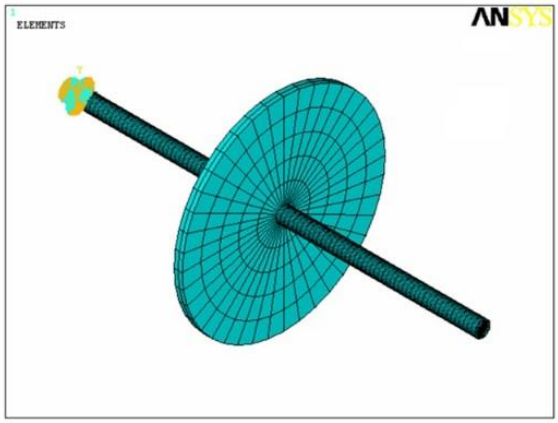

Figure 5. Meshed clamped-free system

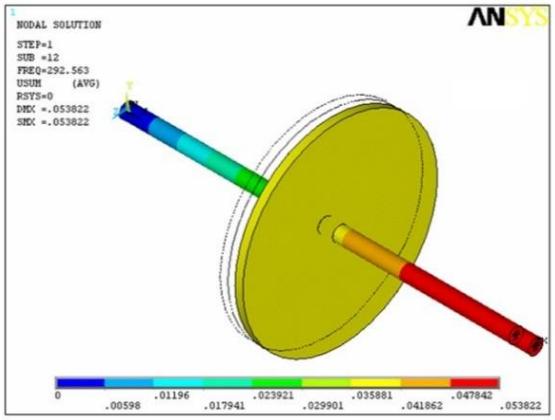

Figure 6. 1st mode shape for clamped-free BCs

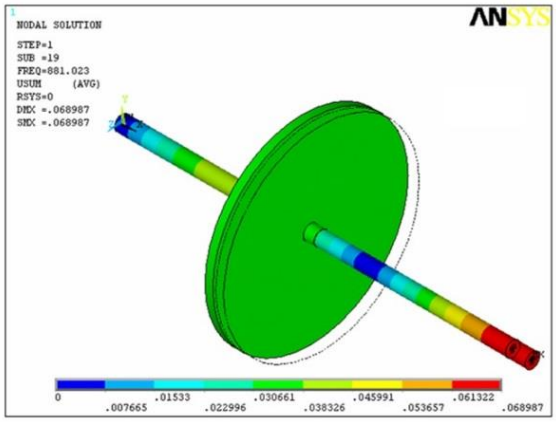

Figure 7. 2nd mode shape for clamped-free BCs

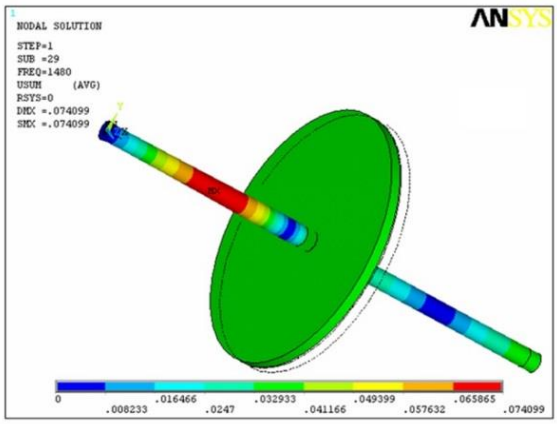

Figure 8. 3rd mode shape for clamped-free BCs

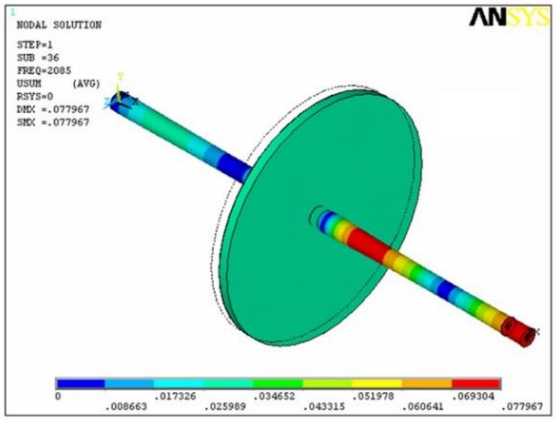

Figure 9. 4th mode shape for clamped-free BCs

According to Table 2, there is less than 2% error between the results of Hybrid modeling method and the results of FEM solution. This example results verify the results of the new method and approve the accuracy of them as well. They also show the simplicity of modeling of structural and industrial systems with any BCs.

4. The Propeller Shaft Analysis

Vibration study of propeller shaft system is very significant in the design of shafts for marine crafts, especially ships. The operating speed of these systems should be kept far from their natural frequencies. Furthermore, any redundant vibration or noise makes clear the position of underwater vehicles and leads to unwanted dangers. According to the significance and wide application of propeller shafts in submarines and ships, developing an accurate method of vibration analysis is of great importance. Hence; the exact methods, such as the DLMT, are more appropriate than the approximate ones, such as the TMM.

4.1. The Distributed- Lumped Modeling Analysis

The propeller shaft system studied in this paper is based on the model presented in Figure 10. In this figure, "D" and "L" refer to the distributed and lumped element, respectively. The geometrical and the physical properties of shaft and disk (propeller model) are presented in Table 3.

Table 3. Properties of the propeller shaft model

Parameter	Quantity
Shaft Overall Length l	7 m
Shaft Diameter d	0.160 m
Density of Shaft Material ρ	7850 kg/m^3
Modulus of Elasticity for Shaft E	210 GPa
Shear Modulus of Shaft G	80 GPa
Flange Thickness t	0.030 m
Propeller Diameter d	0.750 m
Propeller Mass M_{prop}	1250 kg

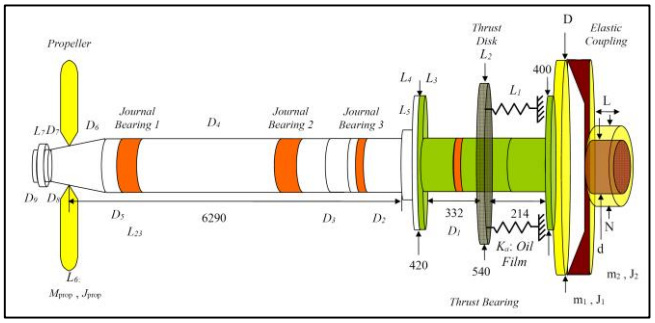

Figure 10. Model of marine propeller shaft system

As shown in Figure 10, the propeller shaft consists of 3 bearings, which has no effect on the axial vibration. There is an oil film between the thrust rotating pads attached to the thrust disk and the bearing housing attached to the main structure. The oil film is modeled as an axial spring with $k_a=5\times10^7$ N/m. the structure is assumed as fixed support here.

The flange coupling consists of 2 disks assumed as lumped element. The propeller is modeled as a disk, in which the thickness and radius is set in such a way that the disk possesses the same mass and moment of inertia as the propeller. The transfer matrix for this system is obtained as follows:

$$[T]=[T_L]_1[T_L]_2[T_D]_1[T_L]_3[T_L]_4[T_L]_5[T_D]_2[T_D]_3 \times[T_D]_4[T_D]_5[T_D]_6[T_L]_6[T_D]_7[T_D]_8[T_L]_7[T_D]_9 \quad (30)$$

The linear spring, which is the representative of oil film; is modeled in the following form:

$$\begin{Bmatrix} p_0 \\ u_0 \end{Bmatrix} = \begin{bmatrix} 1 & 0 \\ 1/k_a & 1 \end{bmatrix} \begin{Bmatrix} p_1 \\ u_1 \end{Bmatrix} \quad (31)$$

Therefore, the system consist of spring (the representative of oil film) and mass (the model of thrust disk) can be displayed as follows:

$$\begin{Bmatrix} p_0 \\ u_0 \end{Bmatrix} = \begin{bmatrix} 1 & 0 \\ 1/k_a & 1 \end{bmatrix} \begin{bmatrix} 1 & -m_d\omega^2 \\ 0 & 1 \end{bmatrix} \begin{Bmatrix} p_2 \\ u_2 \end{Bmatrix} = \begin{bmatrix} 1 & -m_d\omega^2 \\ \dfrac{1}{k_a} & -\dfrac{m_d}{k_a}\omega^2+1 \end{bmatrix} \begin{Bmatrix} p_2 \\ u_2 \end{Bmatrix} \quad (32)$$

Equation (30) is the main equation for longitudinal vibration of the system which relates left and right ends together. The BCs are considered as fixed-free ends which result in the following frequency equation:

$$\begin{Bmatrix} p_0 \\ 0 \end{Bmatrix}_{clamped\ end} = \begin{bmatrix} T_{11} & T_{12} \\ T_{21} & T_{22} \end{bmatrix} \begin{Bmatrix} 0 \\ u_n \end{Bmatrix}_{free\ end} \quad (31)$$

Therefore:

$$T_{22}=0 \quad (32)$$

Table 4 shows the longitudinal natural frequencies of the propeller shaft using the distributed- lumped modeling technique.

4.2. The FEM Analysis

In order to compare and confirm the results, the finite element method is used to investigate the natural frequencies and mode shapes of the propeller shaft. Here, KissSoft software is employed to obtain the frequencies and mode shapes. The propeller and flanges are modeled as disks. Figure 11 shows the model. The natural frequencies obtained by this method are presented in Table 4. The first 5 mode shapes for the system are shown in Figures 12-16. According to Table 4, there is a close agreement between the results of the DLMT and FEM in this case.

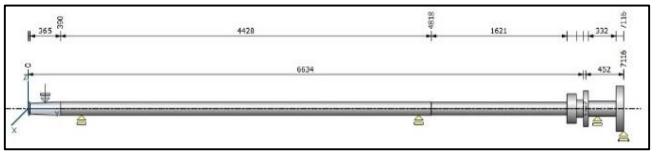

Figure 11. The model and boundary conditions

Table 4. Natural frequencies of the propeller shaft system (Hz).

Frequency Number	DLMT	FEM	%Error (FEM with respect to DLMT)
1	21.4	21.5	0.47
2	199.2	198.6	0.30
3	493.0	492.1	0.18
4	862.3	861.4	0.10
5	1253.2	1249.7	0.28

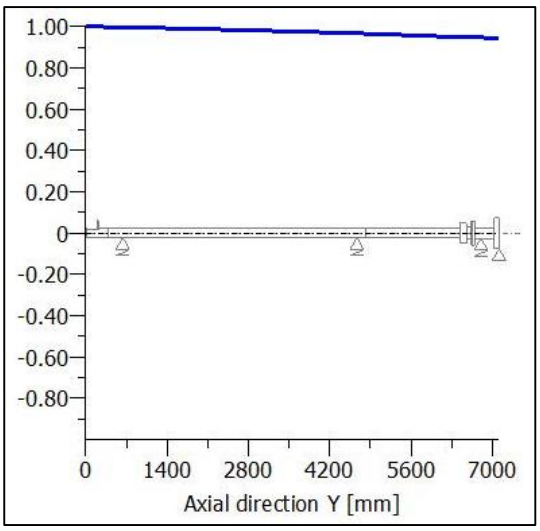

Figure 12. The first mode shape

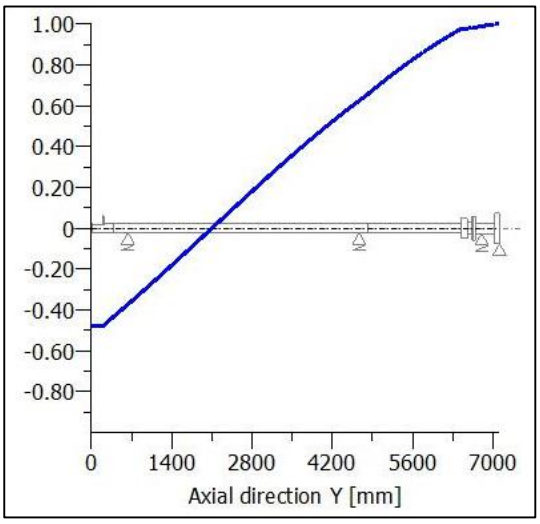

Figure 13. The second mode shape

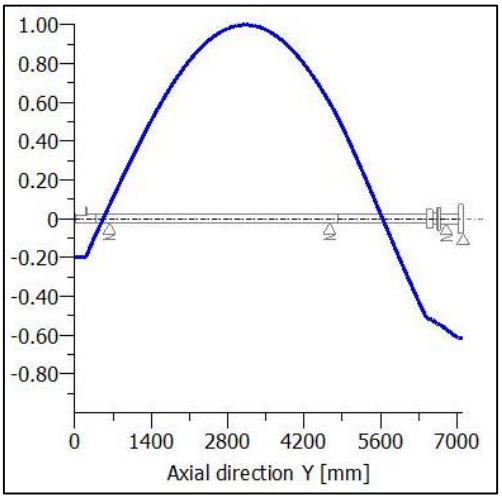

Figure 14. The third mode shape

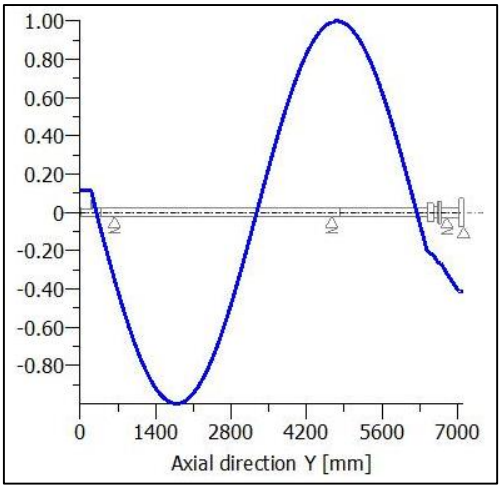

Figure 15. The fourth mode shape

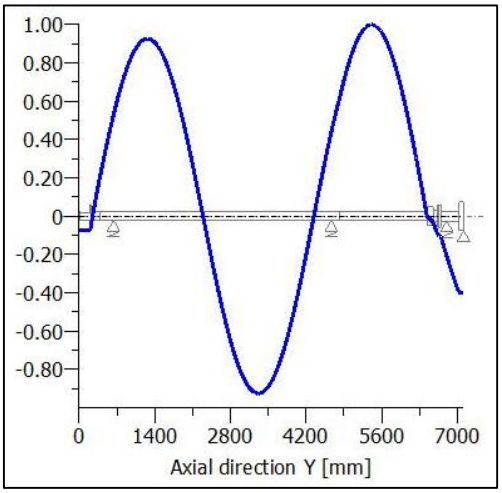

Figure 16. The fifth mode shape

4.3. The Sensitivity Analysis

In this section, the sensitivity analysis for 5 parameters, namely oil stiffness, propeller mass, foundation stiffness, main shaft length and diameter are investigated.

The oil stiffness value is obtained by tribology analysis and relates to the oil film thickness. It is very difficult to determine the exact value of this parameter by solving Reynolds nonlinear fluid equations [13,14]. In order to decrease the transmitted vibrations to the hull, the Resonance Changer (RC) could be utilized [2]. Therefore, the sensitivity analysis can display the significance of oil stiffness value and its effect on the axial frequency values.

Figure 17 shows the first 3 natural frequency changes due to the ±50% variations of oil stiffness value. According to this figure, it can be seen that the oil stiffness value greatly affects the first frequency values of the system (about -30% - +22% variations), while its effect on the higher frequencies are negligible. The basic reason is that the k_a value is very smaller than the shaft stiffness value, and the whole propeller shaft system acts as a mass connected to the spring; while for the higher mode shapes, the shaft itself vibrates and the spring has less effect, conclusively.

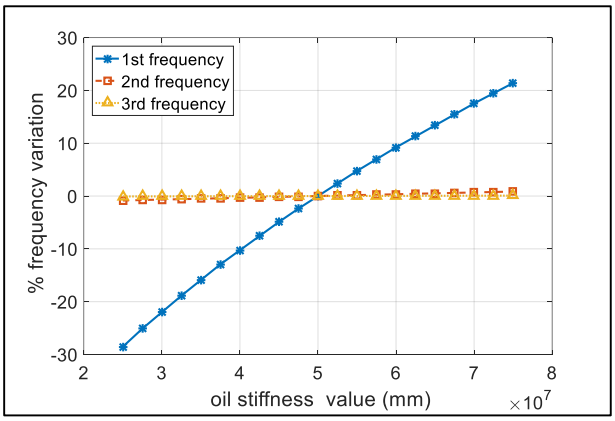

Figure 17. Frequency variation (%) with respect to the oil stiffness changes

Figure 18 shows the effect of ±50% propeller mass variations on the first 3 natural frequencies. It is depicted that the propeller mass value has the most effect on the first frequency value of the system (about +15% - -10% variations), and its effect on the higher frequencies are gradually reduced. It also shows that decreasing the propeller mass brings more frequency changes compared with the increasing of its value.

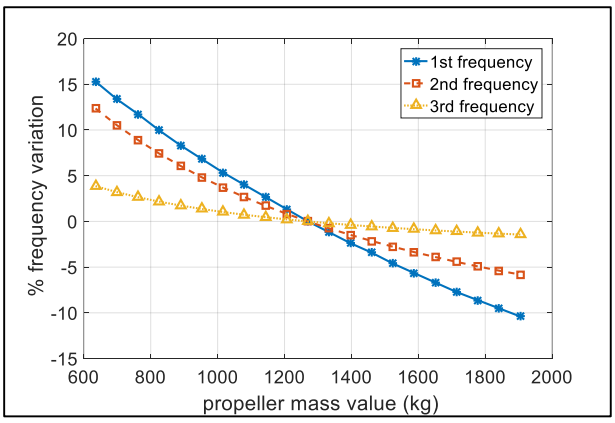

Figure 18. Frequency variation (%) with respect to the propeller mass changes

The effect of main shaft length on the first 3 frequencies are displayed in Figure 19. According to

this figure, ±50% variations of shaft length value changes the first frequency about ±10%, while it alters the third frequency between +75% and -25%. This shows that decreasing the shaft length has more effect on the frequency values in contrast with the increasing of its value.

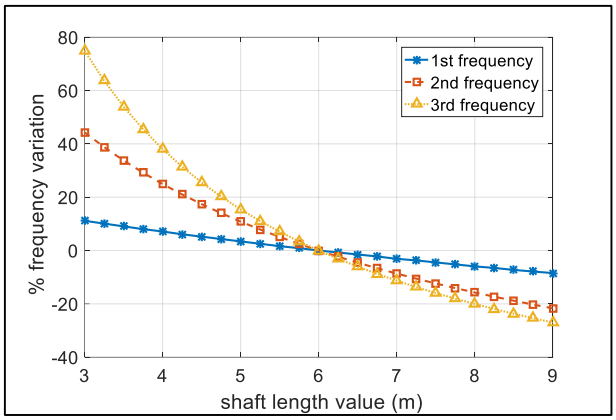

Figure 19. Frequency variation (%) with respect to the shaft length changes

Figure 20 shows the first 3 natural frequency changes due to the ±50% variations of main shaft diameter. According to this figure, it can be seen that the shaft diameter value greatly affects the frequency values of the system (about -40% - +30% variations). It can be seen that increasing the shaft diameter would decrease the first frequency value, and vice versa. For the second and third natural frequencies (and also higher modes) increment of the shaft diameter arises the frequency values, and inversely the diameter reduction would reduce the frequencies. The main reason is that since the oil stiffness value is very smaller than the shaft stiffness value, for the first mode the whole propeller shaft system acts as a mass connected to the spring; while for the higher modes, the shaft itself oscillates and thus the spring has less effect on the mode shape of vibration.

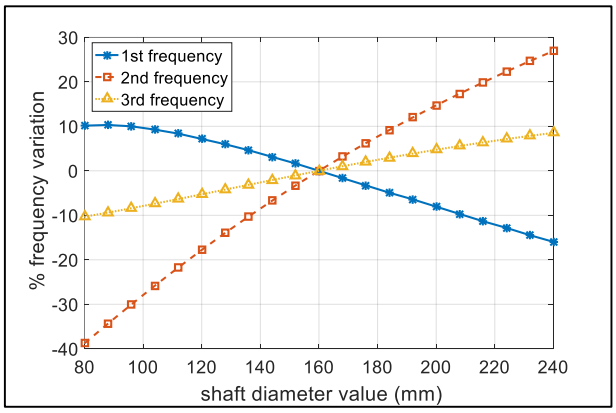

Figure 20. Frequency variation (%) with respect to the shaft diameter changes

The effects of structural stiffness value of thrust bearing foundation on the first 3 natural frequencies are investigated in Figure 21. Since the thrust bearing is attached to the hull through the foundation and supporting structure, the final support of the system is not exactly the fixed one and the foundation could be modeled by a spring [14].

This figure shows that changing the base stiffness value from 10^7 to 10^9 (N/m) brings about -60% to -2% changes of the first natural frequency with respect to the shaft with fixed base foundation. In addition, it can be seen that the base stiffness has negligible effect on the higher frequencies. Therefore, the exact determination of foundation stiffness is so significance.

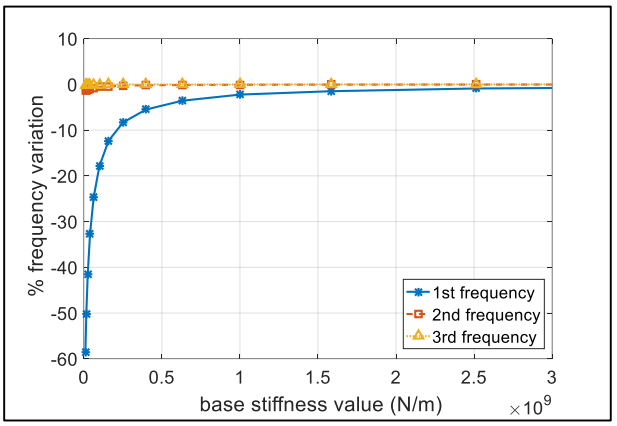

Figure 21. Frequency variation (%) with respect to the base stiffness variations

5. Conclusions

In this paper, the shaft longitudinal equation of motion is solved by the analytical method. Considering the distributed lumped modeling technique (DLMT), the transfer matrix for the distributed element is presented by applying the proposed method. The transfer matrix for the lumped elements is also obtained using hybrid modeling.

The natural frequencies obtained by DLMT is compared and verified with the results of FEM for the rotor shaft with a disk in the middle. The technique is also applied to calculate the frequencies of a marine propeller shaft system modeled as a shaft with different supports carrying propeller and flanges as lumped elements. The frequencies obtained by DLMT are compared with the results of finite element method, using KissSoft software. The mode shapes of the propeller shaft model are also obtained by KissSoft software. As it is shown in Table 4, the two methods are differed less than 1 percent which confirms the DLMT results.

The sensitivity analysis for oil stiffness, propeller mass, foundation stiffness, main shaft length and diameter are also investigated. It is shown that the oil stiffness, the propeller mass and the foundation stiffness have the most effects on the first natural frequency; and the shaft length and diameter have the most effects on the higher frequencies.

The results presented herein show that the natural frequencies and mode shapes of the longitudinal

vibration of a complicated shaft with various supports and flanges can be computed effectively using distributed lumped modeling technique. Moreover, since the method is closely related to the governing partial differential equations for the system, accurate results are achieved. In this way, the simplicity and accuracy of this method brings proper application for the complicated systems.

6. References

1- Randall, R.B., (2011), *Vibration- Based Condition Monitoring: Industrial, Aerospace and Automotive Applications*, John Wiley & Sons Inc., USA.

2- Soheili, S., Ghasemizadeh P., and Hosseini, E., (2020), *Design of Vibration Reducer for Thrust Bearing of Marine Shaft*, Journal of Marine Engineering, Vol. 16 (32), p. 131-140.

3- Halilbese, A., Ozsoysal, O. A., (2021), *The Coupling Effect on Torsional and Longitudinal Vibrations of Marine Propulsion Shaft System*, Journal of ETA Maritime Science, Vol. 9(4), p. 274-282.

4- Xiang, L., Yang S., Gan, C., (2012) *Torsional Vibration of a Shafting System under Electrical Disturbances*, Shock and Vibration, Vol. 19, p. 1223–1233.

5- Hussain Aboud, A.A., Khalaf Ali, J., (2021), *Study of Effective Parameters in Stability and Vibration of Marine Propulsion Shafting Systems*, Journal of Physics: Conference Series, Vol. 1973 (012032), doi: 10.1088/1742-6596/1973/1/012032.

6- Whalley, R., (1988), *The Response of Distributed-Lumped Parameter Systems*, Proceedings of IMechE, Vol. 202(C6), p. 421-428.

7- Aleyaasin, M., Ebrahimi M. and Whalley, R., (2001), *Flexural Vibration of Rotating Shafts by Frequency Domain Hybrid Modeling*, Journal of Computers and Structures, Vol. 79, p. 319-331.

8- Soheili S. and Abachizadeh, M., (2022), *Flexural Vibration of Multistep Rotating Timoshenko Shafts Using Hybrid Modeling and Optimization Techniques*, Journal of Vibration and Control, doi: 10.1177/10775463211072406.

9- Tahani, M., Soheili, S., Abachizadeh, M. and Farshidianfar, A., (2008), *Rotors Frequency and Time Response of Torsional Vibration Using Hybrid Modeling*, Proceeding of 16th Annual Mechanical Engineering Conference (ISME), Kerman.

10- Soheili, S. and Abachizadeh, M., (2023), *Flexural vibration of multistep rotating Timoshenko shafts using hybrid modeling and optimization techniques*, Journal of Vibration and Control, Vol. 29(7-8), p. 1833–1849.

11- Rao, S.S., (2016), *Mechanical Vibration*, 6th Edition, Pearson Publications, USA.

12- Meirovitch, L., (2001), *Fundamentals of Vibration*, McGraw-Hill Inc., Singapore.

13- Chu, W., Zhao, Y., Zhang, G., and Yuan, H., (2022), *Longitudinal Vibration of Marine Propulsion Shafting: Experiments and Analysis*, Journal of Marine Science and Engineering, Vol. 10(1173), https://doi.org/ 10.3390/jmse10091173.

14- Zhang, G., Zhao, Y., Li, T., and Zhu, X., (2014), *Propeller Excitation of Longitudinal Vibration Characteristics of Marine Propulsion Shafting System*, Shock and Vibration, Vol. 2014, p. 1-19, http://dx.doi.org/10.1155/2014/413592.